Highlights of Spanish Astrophysics XII, Proceedings of the XVI Scientific Meeting of the Spanish Astronomical Society held on July 15 - 19, 2024, in Granada, Spain. M. Manteiga, F. González Galindo, A. Labiano Ortega, M. Martínez González, N. Rea, M. Romero Gómez, A. Ulla Miguel, G. Yepes, C. Rodríguez López, A. Gómez García and C. Dafonte (eds.), 2025

J-PLUS-based spatially resolved emission line and stellar population properties in nearby galaxies in groups

Thainá-Batista, J.[1,2], Cid Fernandes, R.[2], and González Delgado, R. M.[1]

[1] Instituto de Astrofísica de Andalucía (CSIC), PO Box 3004, 18080 Granada, Spain
[2] Departamento de Física, Universidade Federal de Santa Catarina, PO Box 476, 88040-900 Florianópolis, SC, Brazil

Abstract

We present the first results on the stellar and nebular properties of two nearby galaxy groups, M101 and M51, using data from the J-PLUS (Javalambre Photometric Local Universe Survey). Our goal is to explore the properties of individual galaxies within these groups and compare them. We developed a robust pre-processing pipeline to enhance the data quality, ensuring more reliable results. To derive the properties, we used the AlStar code and we presented two examples of fit and maps of the stellar mass surface density, the mean stellar age, and the equivalent width of Hα.

1 Introduction

Studying galaxy groups is important for understanding the role of the environment in galaxy formation and evolution. Galaxy groups represent intermediate environments between isolated galaxies and clusters, are denser structures that can contain hundreds to thousands of galaxies.

Here we present the first results for the M101 and M51 galaxy groups, but a detailed result and analysis are ongoing work and will be published soon (Thainá-Batista in preparation).

2 Data and pre-processing

The data used in this work come from the Javalambre-Photometric Local Universe Survey (J-PLUS), an ongoing project that uses an 80 cm robotic telescope in the Observatorio Astrofísico de Javalambre (OAJ), in Spain. J-PLUS employs 12 filters, with an image pixel

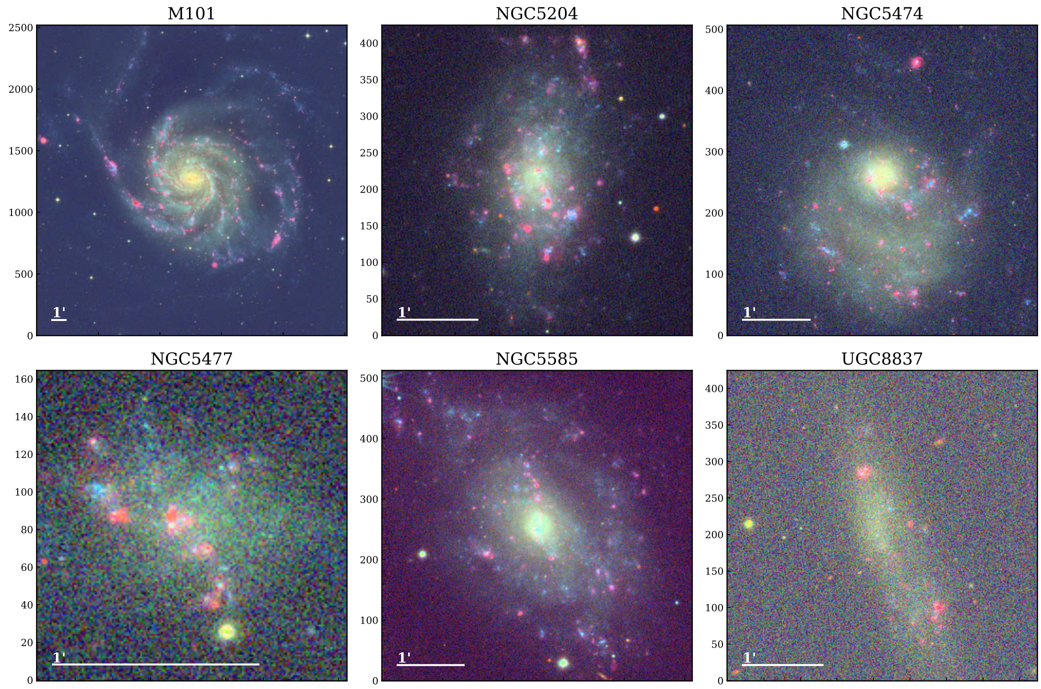

Figure 1: RGB composites of the galaxies of M101 group, using J0660, g, sum of five bluer filters in the channels (r, g, b) of the original data. The white line represents the 1 arcmin ($\sim$ 1 kpc) distance.

scale of 0.55 arcsec, with five broad and seven narrow band filters, covering the $\sim$ 3500–9000 Å wavelength range. A complete description is found in [5].

2.1 Sample

The sample is composed of two galaxy groups: M101 and M51. Both groups present spiral and irregular galaxies, from large ones to dwarfs, all of them with HII regions.

Fig. 1 shows RGB images of the six galaxies that form the M101 group. M101 itself is the largest and the main galaxy of the group with a diameter of nearly 30 arcmin in diameter. At a distance of just 7.11 Mpc, M101 is a lopsided spiral (SAB(rs)cd), and exhibits tidal effects. NGC5477, on the other hand, is a dwarf galaxy with a diameter of less than 1 arcmin. The other four galaxies vary in size from $\sim$ 4 to 8 arcmin. Therefore, the group has a diameter size range from $\sim$ 34 kpc (for M101), to 1 kpc (for the smaller galaxy, NGC5477).

The M51 group has eight galaxies that are shown in Fig.2. The main galaxy of the group is M51, which is a pair of galaxies at a distance of 8.59 Mpc. It has visible structures of dust, as also seen in M63. These are the two largest galaxies of the group, which also included systems as small as UGC08215. This group has a diameter size range from $\sim$ 9 arcmin (12 kpc) to $\sim$ 0.5 arcmin (687 kpc).

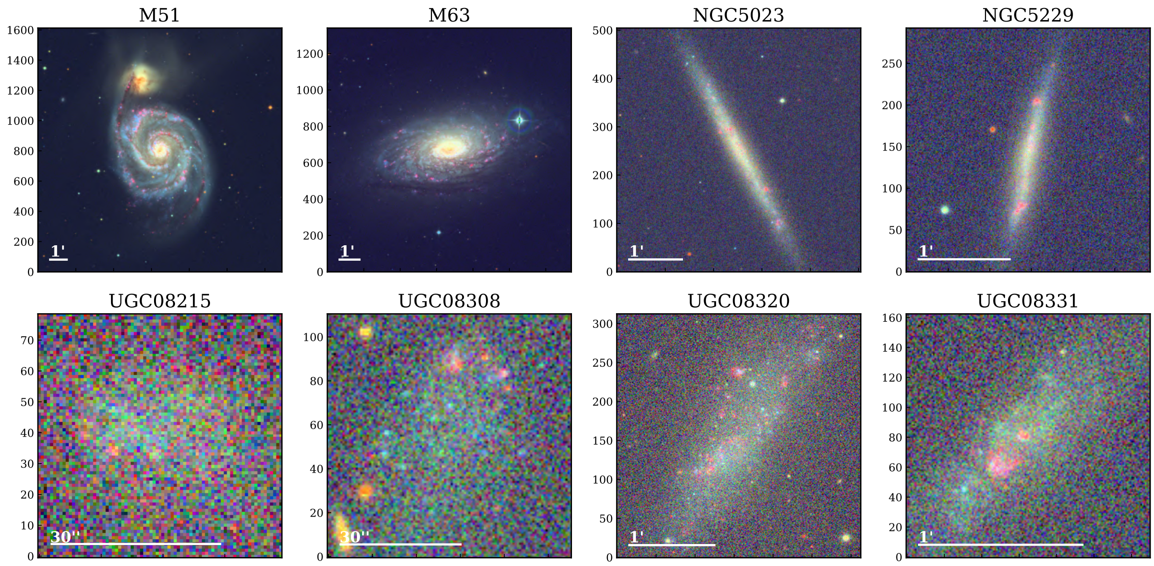

Figure 2: The same that Fig. 1 but for M51 group. Where 1 arcmin is ~ 1.3 kpc.

2.2 Pre-processing

After extensive tests and analyses, we developed a sequence of pre-processing steps in the cubes. The first part consists of producing some masks, the star mask that is made using some tools of the photutils [1], then a contour galaxy mask. So, in the second part, we apply some filters and binnings to improve the signal-to-noise. Fig. 3 shows how the data changes after each step of pre-processing for the u and r bands. In the first column we show (1) the original data. Then we apply (2) a Butterworth filter, (3) PSF homogenization (that consists of degrading the filters to the worst PSF), (4) 2×2 binning, and, finally, (5) Voronoi binning [3] based on the u band.

Fig. 3 shows the importance of doing these pre-processing to get reliable results, the x-axis shows the numbers of the total of pixels with negative fluxes decreasing after each step until get zero. The larger difference occur in the bluer bands, which are where we have more relevant information for stellar population work, like the 4000 Å break.

3 Method

To estimate stellar populations and the emission lines properties we use the spectral synthesis code AlStar. From previous work ([8]), we already have tested AlStar on the J-PLUS filter system, obtaining good results for all properties when compared spectroscopic-based estimates.

To fit the multi-band photometry we use an updated version of the models [2]. The stellar base is composed by 5 metalicities from $Z = 0.24$ to $3.5 Z_{\odot}$, and 16 ages, from $t = 1$ Myr

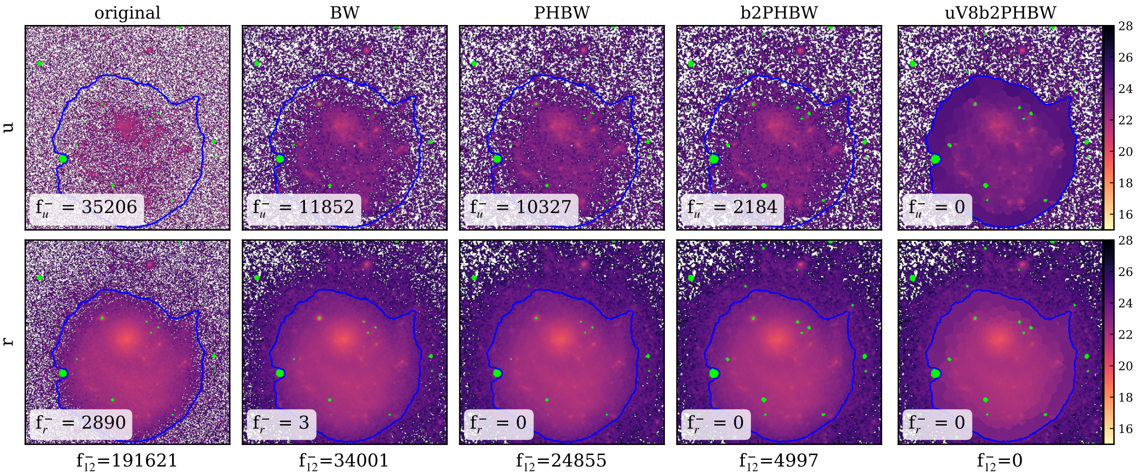

Figure 3: Example of the step-by-step of the pre-processing performed to the NGC 5574. The blue line represents the contour of the galaxy mask. The first and second rows are the map of the magnitude/arcsec^2 in the u and r-band respectively. The legend shows the number of negative fluxes inside the galaxy mask in the u and r bands, and the x-axis is the sum of the negative fluxes in all 12 bands for each step of pre-processing. The green circles are the masked stars.

to 14 Gyr. To account for emission lines we use an empirically-defined nebular base of 94 components, with five groups of lines: [O II]$\lambda\lambda3727$, [O III]$\lambda\lambda4959, 5007$, [N II]$\lambda\lambda6548, 6584$, [S II]$\lambda\lambda6717, 6731$, and the Balmer series (from Hα to Hϵ). The treatment of dust is with a differential extinction and the reddening law used is that from [4]. The initial mass function is from [6].

4 Results

Before analyzing the parameters obtained, we need to check the quality of the fits. Fig. 4 shows two examples of an AlStar fit to the external faint pixels of M51. Maps for the main galaxies from each group are presented in Figs. 5 and 6. Comparing the maps of stellar mass density, we can see that the nucleus of M51 is ~ 10 times denser than in M101. Figs. 5 and 6 show a good relation to the structures of young populations and stronger line emission, i.e. between the maps of mean age ($\langle \log t \rangle_{Flux}$) and the equivalent width of Hα ($W_{H\alpha}$) for both galaxies. These and other stellar population and emission line maps, as well as azimuthally averaged radial profiles will be presented in an upcoming publication.

5 Summary and Perspectives

We have built a consistent pre-processing pipeline for J-PLUS data, which visibly and quantitatively improves the signal-to-noise ratio, ensuring trustworthy results. The code AlStar

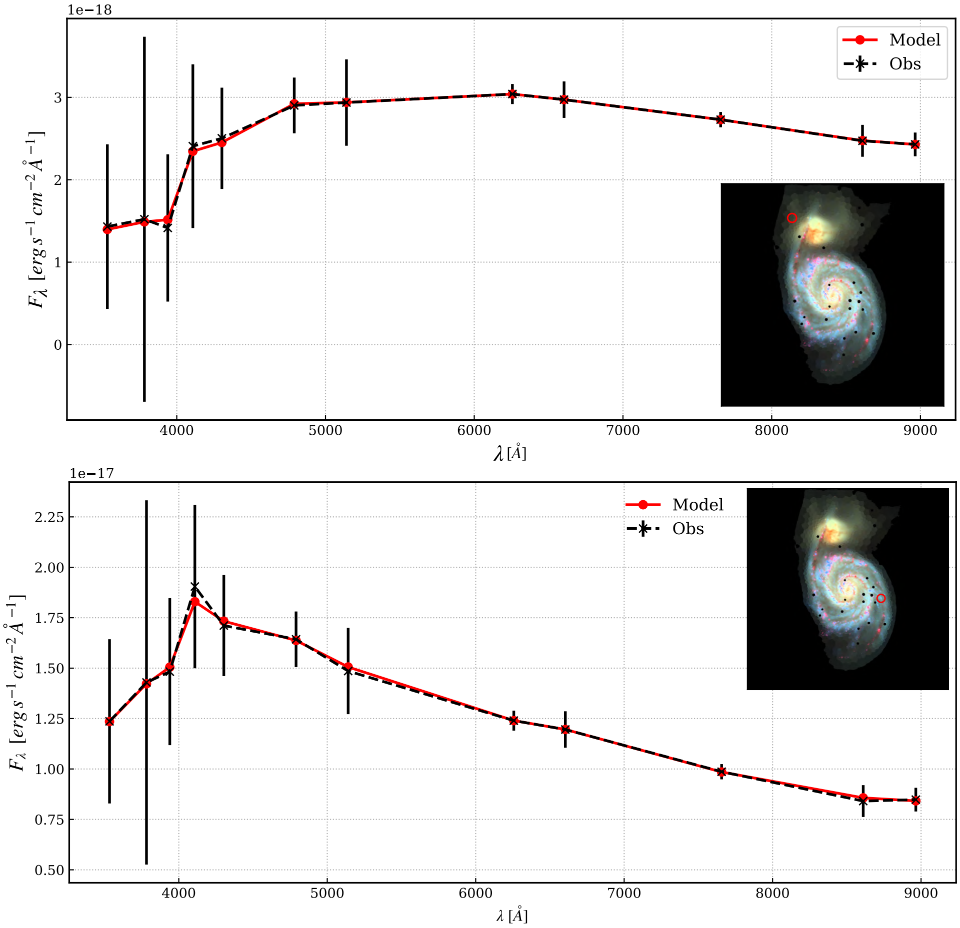

Figure 4: Example of two fits from AlStar to the external pixels of M51 galaxy, shown in the red circle in the RGB image. The black-dashed line is the observed data and the red line is the model.

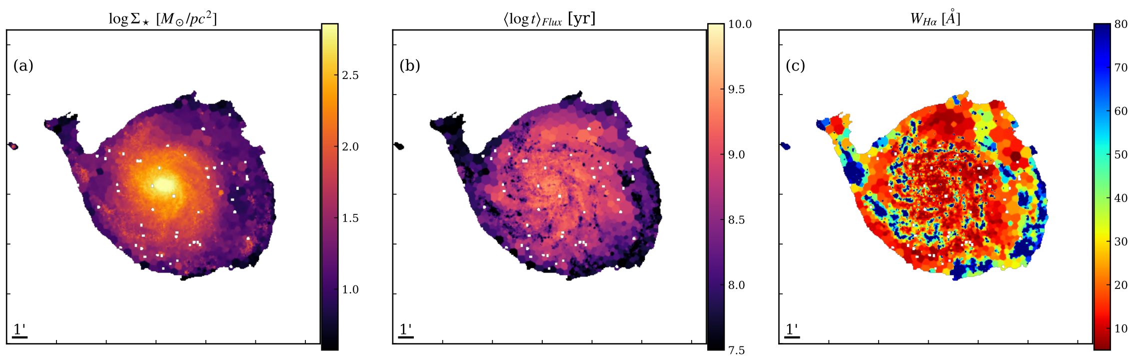

Figure 5: AlStar-based maps for M101: (a) stellar mass density surface ($\log \Sigma_\star$), (b) average of the log age weighted by flux, and (c) equivalent width of Hα.

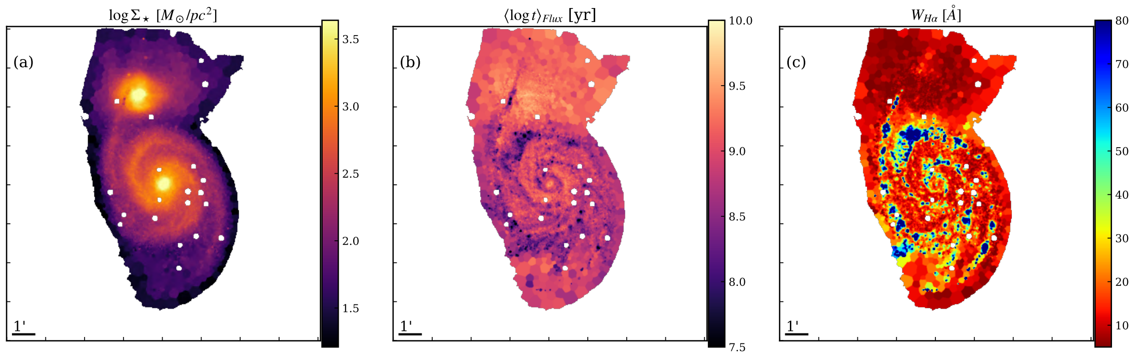

Figure 6: As Fig.5, but for M51.

demonstrates good performance for both stellar and nebular property analyses, showing consistent agreement between them. The preliminary results suggest that there is promising work to be done on the comparison of the galaxy groups.

Acknowledgments

The authors acknowledge financial support from CAPES, 88881.892595/2023-01.

References

[1] Bradley, L., Sipőcz, B., Robitaille, T., et al. 2024, astropy/photutils: 1.12.0

[2] Bruzual, G. & Charlot, S. 2003, MNRAS, 344, 1000

[3] Cappellari, M. & Copin, Y. 2003, MNRAS, 342, 345

[4] Calzetti D., Armus L., Bohlin R. C., Kinney A. L., Koornneef J., Storchi-Bergmann T., 2000, ApJ, 533, 682

[5] Cenarro, A. J., Moles, M., Cristóbal-Hornillos, D., et al. 2019, Astronomy & Astrophysics, 622, A176

[6] Chabrier G., 2003, Publications of the Astronomical Society of the Pacific, 115, 763–795

[7] Karachentsev I. D., Karachentseva V. E., Huchtmeier W. K., Makarov D. I. 2004 AJ 127, 2031 – A C

[8] Thainá-Batista, J., Cid Fernandes, R., Herpich, F. R., et al. 2023, MNRAS, 526, 1874